Developmental Biology **240,** 488–498 (2001)
doi:10.1006/dbio.2001.0436, available online at http://www.idealibrary.com on IDEAL®

Germ Cell Migration

Kathleen A. Molyneaux, Jim Stallock, Kyle Schaible, and Christopher Wylie[1]

Division of Developmental Biology, Children's Hospital Research Foundation, Cincinnati, Ohio 45229

In mouse embryos, the primordial germ cells arise during gastrulation prior to, and distant from, the prospective gonads. Observations of PGCs in culture, and in fixed sections, have suggested, but not proved, that they migrate to the gonad by a process of active migration. The opaque nature of the early mouse embryo has precluded direct observation. Using confocal microscopy, we have filmed living PGCs expressing eGFP in tissue slices from mouse embryos at different stages of development. We find four clearly distinct phases of PGC migration. First, until E9.0–E9.5, PGCs are already highly motile, but do not leave the gut. Second, in the E9.0–E9.5 period, before the mesentery forms, PGCs very rapidly exit the gut, but do not migrate towards the genital ridges. Third, during the E10.0–E10.5 period, PGCs migrate directionally from the dorsal body wall into the genital ridges. In contrast to the prevailing model of germ cell migration, very few, if any, PGCs found in the gut mesentery at E10.5 migrate into the genital ridges. Finally, at E11.5, PGCs are slowing and the direction of movement is dependent on the sex of the embryo. This allows, for the first time, a formal description of the events of PGC migration in the mouse.

Key Words: **germ cells; migration; mouse.**

INTRODUCTION

In the mouse embryo, primordial germ cells arise during gastrulation in the posterior primitive streak. The somatic cells of the gonad arise approximately 48 h later, from the intermediate mesoderm, and from the genital ridges, which are on the dorsal body wall of the embryo, lateral to the root of the hind-gut mesentery. In their route to the genital ridges, the germ cells occupy sequentially the definitive endoderm (E7.5), the hind-gut epithelium (E8.0–E9.0), and the mesentery of the hind-gut and dorsal body wall mesenchyme (E9.5–E10.5). Most of the germ cells are in the genital ridges at E11.5, although a significant proportion remains scattered along the migratory route, and are regarded as ectopic.

The degree to which germ cells are motile during these different phases is not precisely known, and has been inferred from their shapes and positions in fixed tissue, using histochemical and antibody markers, or observation of PGCs explanted into culture. Individual PGCs explanted from E8.5 to E10.5 have been shown to be motile in culture (Stott and Wylie, 1986). However, the degree to which this occurs *in vivo* is not known, and the direction and speeds seen *in vitro* do not necessarily reflect the *in vivo* situation. PGCs explanted onto feeder layers from E10.5 embryos extend processes and appear elongated in culture, a property which is lost in PGCs explanted from later embryos (Donovan *et al.*, 1986). Cell shape in fixed tissue has also been used to suggest that PGCs may be motile in the hind-gut (Clark and Eddy, 1975). During E10.5 to E11.5 a progressive change in cell shape takes place. PGCs in the hind-gut mesentery at E10.5 extend long processes, which in many cases touch other germ cells and appear to link them into a network. By E11.5, most of these processes have gone, and the PGCs are in tightly coherent groups (Gomperts *et al.*, 1994). This suggested that cell:cell attachment and subsequent aggregation may play a role in the coalescence of PGCs into the genital ridges (Gomperts *et al.*, 1994). However, in the absence of dynamic studies, it is not known to what extent PGCs move as individuals or as a connected group.

The degree to which PGCs move directionally towards the genital ridges at any of these stages is unknown, as is

Supplementary data for this article are available on IDEAL (http://www.idealibrary.com)

[1] To whom correspondence should be addressed. Fax: 513-636-4317. E-mail: wylv9m@chmcc.org.

0012-1606/01 $35.00

the mechanism of PGC directionality. Germ cell accumulation in the genital ridges can be explained by three general mechanisms, none of which have been formally excluded. First, germ cells could migrate randomly, and be trapped upon contact with the somatic cells (or matrix) in the genital ridges. Large numbers of germ cells do not reach the genital ridges, so this is a tenable hypothesis. Second, germ cells could migrate in a vectorial manner towards the genital ridges, and be arrested by contact with the somatic gonad. Third, germ cells could be pushed into the genital ridges by morphogenetic movements of tissues around them. Since PGCs have been shown to be capable of motility in culture, this hypothesis has been less accepted, but remains a formal possibility.

The only way to answer the many questions about PGC migration is to directly observe them in the living embryo. To this end, we have used a line of mice expressing green fluorescent protein (GFP) in the early germ line cells (Anderson *et al.*, 1999). We have cultured slices of living embryo at each stage of migration, and made time-lapse movies of germ cell movements over periods of 8–12 h. We find that PGCs in slice cultures obey the spatial and temporal constraints observed *in vivo*, which gives confidence that the movements seen are an accurate reflection of those occurring *in vivo*. In these movies, PGCs can be seen actively moving into the genital ridges at the normal time. We describe quantitatively their rate and directionality of movement at each stage, which allows, for the first time, a formal description of the events of PGC migration. Although this does not explain the molecular mechanism of PGC migration, it does eliminate some of the possible mechanisms listed above, and so restricts the possibilities. It also corrects some misconceptions; the most important of which is that PGCs do not migrate to any significant extent in the hind-gut mesentery. The overwhelming majority of PGCs have migrated from the gut into the dorsal body wall before the mesentery forms. This description will also provide an important framework for the analysis of mutations that affect germ cell migration.

MATERIALS AND METHODS

Mice

All embryos analyzed in this work were generated by crossing CD1 females (Charles River Laboratory) with Oct4ΔPE:GFP homozygous males established on the FVB background (Anderson *et al.*, 1999). These embryos are heterozygous for the Oct4ΔPE:GFP transgenic array and express GFP in the germ cell lineage. Staging of embryos was determined by the appearance of a vaginal plug with E0.5 assumed to be noon of the day on which the plug was noted.

Organ Culture

Embryos were dissected free of the uterus and extraembryonic membranes in PBS + 2% FCS and were transferred to Hepes-buffered DMEM/F-12 media (Gibco BRL) + 15% FCS (DF-12 media). Slices were cut with a scalpel, or where indicated, with a vibrotome. For vibrotome sectioning, we used a modification of a protocol previously used to cut hind-brain slices for studying neural crest migration (Krull and Kulesa, 1998). Briefly, the trunk and tail of the embryo was embedded in 7.5% low melt agarose (Sigma) prepared in DMEM/F-12 media. The tissue-containing block was mounted on a support block of 5% agar and 200-μm-thick sections were cut with a 1000 Classic C vibrotome (Harvard Apparatus) (amplitude 6, speed 4). Slices were placed in millicell CM organ culture chambers (Millipore) precoated with mouse Collagen IV (Becton Dickinson). Organ culture chambers were placed into 50-mm glass-bottom culture dishes (Willco Wells, the Netherlands) and the dishes were filled with DF-12 media up to the level of the organ culture membrane (~3.5 ml). Filming was

FIG. 1. E9.0 PGCs are motile within the hind-gut. (A) A Single confocal image taken in the saggital plane of the trunk of an E9.0 embryo heterozygous for the Oct4ΔPE:GFP transgenic array. Dashed lines indicate the boundary of the hind-gut. "Ant." indicates the anterior and "Vent." the ventral axis of the explant. The tissue was cultured for 8 h and cell movements were filmed as described. (B) Cell movements within the boxed region shown in (A). Green outlines represent the starting positions of cells and red outlines are the final positions of cells. Ten cells were traced within this slice and their paths are shown in black. A black dot marks the starting position of each cell that was traced. Note that cells frequently change their direction of migration at this stage (arrow). (C) A single confocal image taken in the transverse plane of a tissue slice cut by vibrotome from the trunk of an E9.0 embryo. "Dor." indicates the dorsal and "Lat." the lateral axis of the explant. This slice was cultured for 8 h and cell movements were filmed. (D) Line traces showing the movement of cells within the boxed region of (C). (E) A transverse image taken of a tissue slice cut by vibrotome from the trunk of an E9.0 embryo. (F) The slice shown in (E) after 17 h in culture. The position of somites (s), neural tube (n), notochord (no), and lumen of the hind-gut (g) are indicated. Scale bars, 58 μm.

FIG. 2. PGCs emerge from the hind-gut between E9.0 and E9.5. (A) A single confocal image taken in the saggital plane of the trunk of an E9.5 embryo. The walls of the hind-gut are marked by dashed lines. "Ant." marks the anterior and "Vent." the ventral axis of the explant. This specimen was filmed for 8 h and cell movements are shown in (B). Arrows in (B) indicate cells that emerged from the hind-gut into the body wall. (C) A single confocal image taken in the transverse plane of a tissue slice cut by vibrotome from the trunk of an E9.5 embryo. "Dor." marks the dorsal and "Lat." the lateral axis of the explant. This slice was filmed for 8 h and cell movements are shown in (D). Arrows in (D) indicate cells that emerged from the hind-gut into the body wall. (E) A transverse image of a living E9.0 vibrotome slice. Arrow marks a cell extending a process along the basal side of the gut. (F) A transverse image of a living E9.5 vibrotome slice. Arrow marks a cell extending a process away from the gut. The position of somites (s), neural tube (n), notochord (no), aorta (a), and lumen of the hind-gut (g) are indicated. Scale bars, 58 μm.

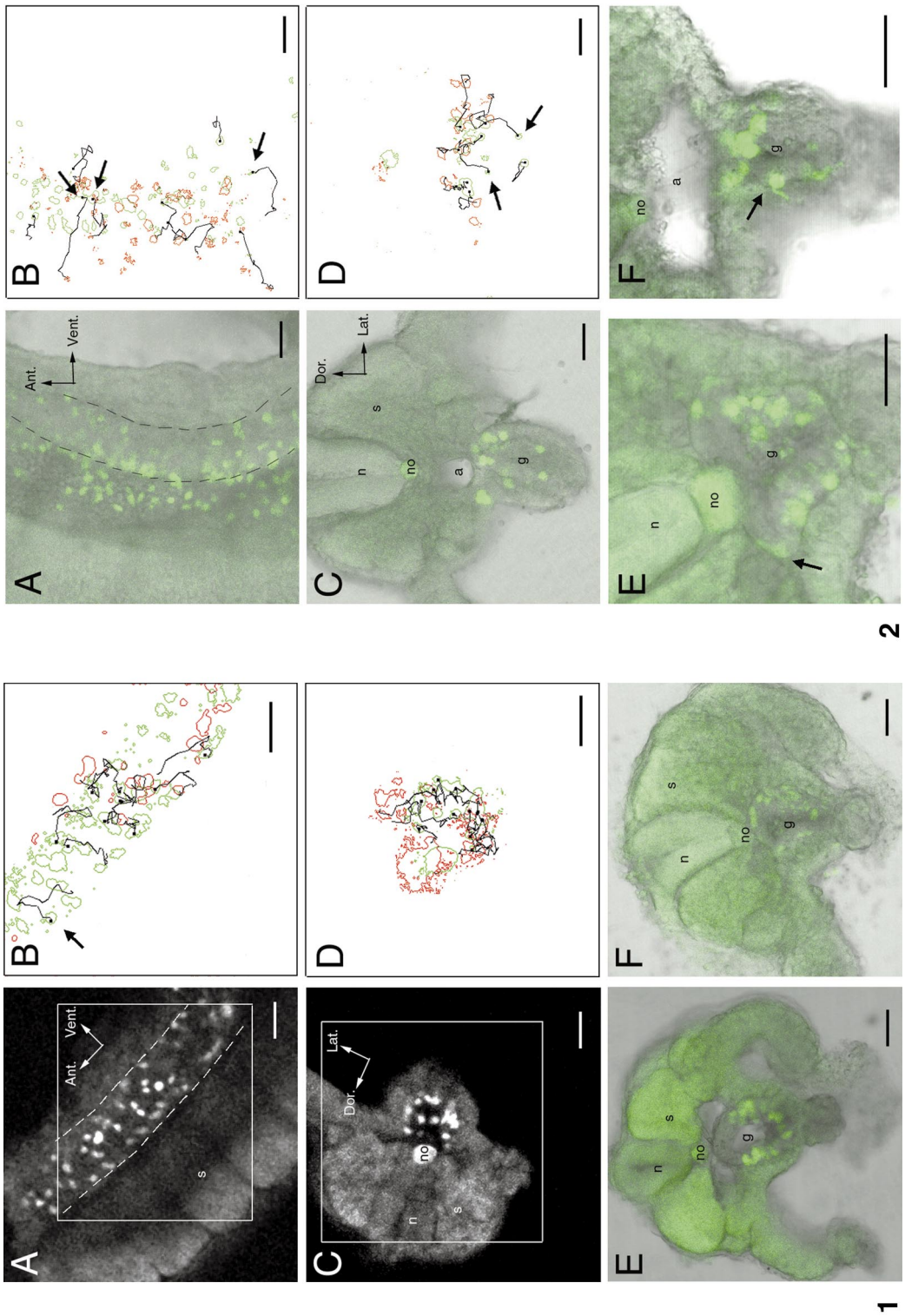

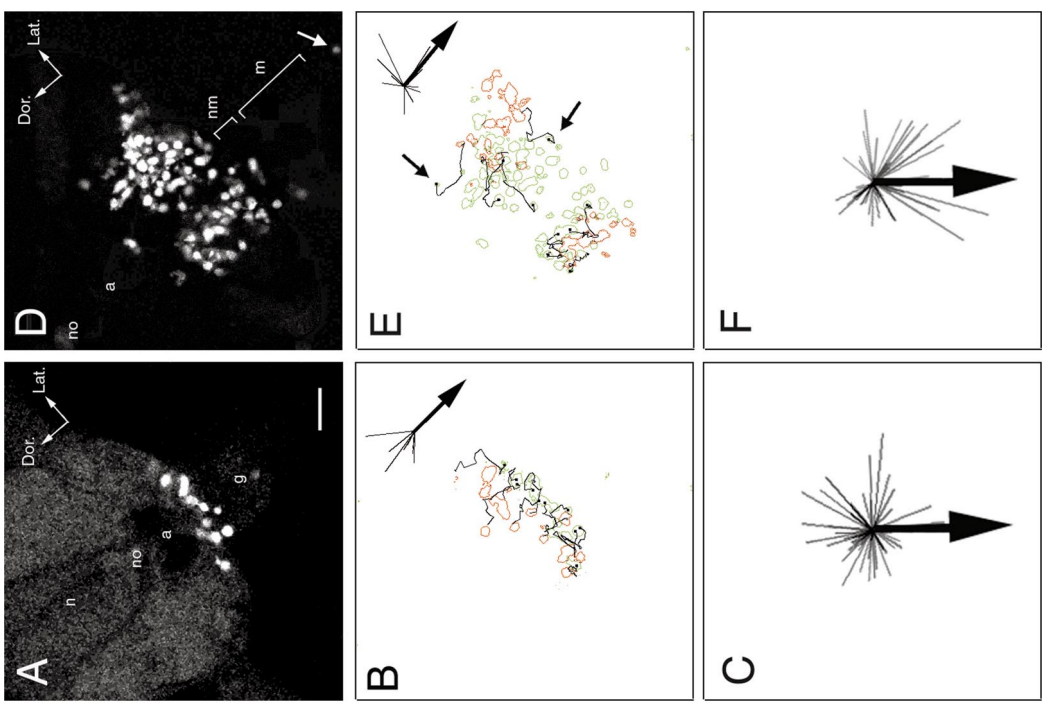

3

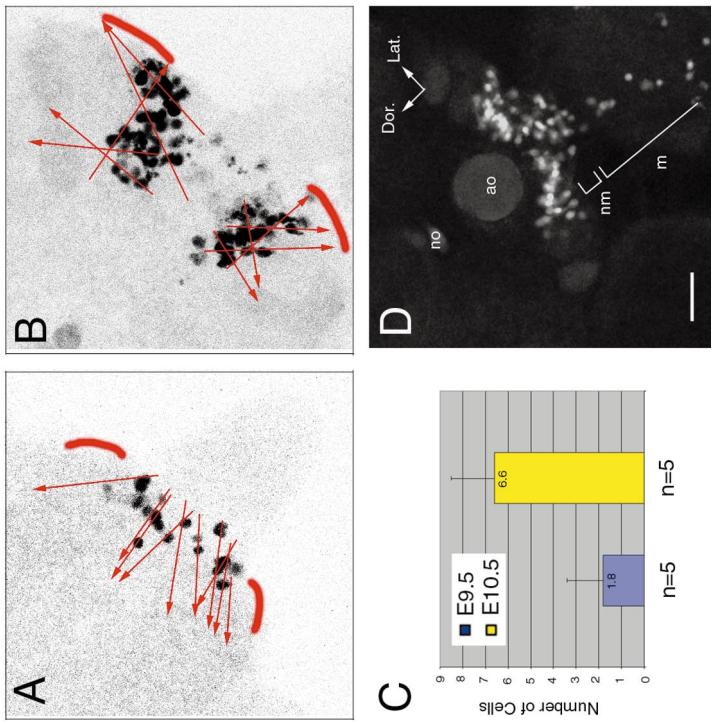

4

performed by using the Zeiss LSM510 confocal system attached to a Zeiss axiovert inverted scope. Images were captured every 5 min for 8–12 h. During filming, dishes were maintained at 37°C by using a heating stage (Zeiss) and humidity was maintained by placing wet paper towels around the stage and covering both towels and dish with the lid from a 100-mm culture dish.

Where indicated, the gender of an explant was confirmed by PCR for SRY (Hogan *et al.*, 1994).

Image Analysis

Movies were exported as stacks of TIFF files and image processing was performed by using NIH Image (http://rsb.info.nih.gov/nih-image/index.html) and Adobe Photoshop (Adobe Systems Incorporated). To perform cell tracing and velocity measurements, a macro was written for NIH Image. Using this macro, the position of a given cell was manually determined at 25-min (5-frame) intervals and these points were connected to generate a line trace. Velocity measurements were generated for each 25-min (0.417-h) interval by using the formula $V = [\text{sqrt}\ (dx^2 + dy^2)](p)/0.417$ h, where dx is the change in the x-axis, dy is the change in the y-axis, and p is the pixel size in μm. Typically, for a 100-frame movie, 19 velocity measurements were generated per cell and these velocities averaged to obtain an overall velocity for that cell. Additionally, the fastest of the 19 measurements was recorded as the maximum velocity for a given cell. The overall velocities and maximum velocities of 10 (E9.0–E10.5) or 20 (E11.5–E12.5) cells were averaged to obtain an average overall and average maximum velocity for each movie. The 10 cells traced were chosen based on 2 criteria. First, only cells that could be unambiguously followed through the entire film were traced. Second, widely separated cells were chosen in order to give a random sampling of possible starting positions. Typically, 25% of cells were untraceable based on the first criteria. At E9.0–E10.5, 10 cells represent approximately 30% of the potentially traceable population and, at E11.5–E12.5, 20 cells represent 20% of the potentially traceable population. Windrose diagrams were also generated by using a macro written for NIH Image. Briefly, the starting and ending positions of each cell were manually determined and these positions were connected by a line representing the net trajectory of a given cell. The net trajectory of each cell traced was then projected onto a common origin to form a windrose diagram displaying the overall angles of movement for a given experiment.

RESULTS

PGCs Are Motile Within the Hind-Gut at E9.0

At E9.0, the head, forelimb buds, and one flap of lateral epidermis were dissected away and the exposed trunk and tail of the embryo was cultured to visualize PGC behavior. Figure 1A shows a single confocal image taken in the saggittal plane parallel to the anterior–posterior (AP) axis of a representative specimen. A movie of 8 h of development of this specimen is provided as supplementary data (movie 1A). When filmed with this orientation, PGC movements along the anterior–posterior (AP) and dorsal–ventral (DV) axes were detected and quantitated; however, movement along the medial–lateral (ML) axis resulted in some PGCs moving out of focus and such cells were not traced. Figure 1B shows cell movements within this specimen. Green outlines represent the starting positions of cells and red outlines are the ending positions of cells. These outlines were generated by applying the trace contour filter from Adobe Photoshop (Adobe Systems Incorporated) to the first and last frames of the movie. Not all cells are reliably defined by this filter (e.g., dim cells), but this serves as a way of presenting the overall movements that occurred within

FIG. 3. The angle of PGC migration changes between E9.5 and E10.5. (A) A transverse image of a living E9.5 vibrotome slice. "Dor." marks the dorsal and "Lat." the lateral axis of the explant. (B) This slice was filmed for 8 h and cell movements are shown. A windrose diagram displaying the angle of movement for each cell traced is shown as an insert in (B). In the windrose, the large arrow indicates the ventral axis (e.g., position of the gut). (C) A composite windrose displaying the angles migrated by cells traced in five E9.5 movies (10 cells per movie). Each individual windrose was aligned with respect to the ventral axis (large arrow). (D) A transverse image of a slice cut by hand from the trunk of an E10.5 embryo. "Dor." marks the dorsal and "Lat." the lateral axis of the explant. Arrow indicates a germ cell in the far mesentery that disappeared during filming. (E) This explant was filmed for 12 h and cell movements are shown. Arrows in (F) indicate two cells converging on the genital ridge from widely divergent starting positions. A windrose displaying the angle of movement for each cell traced is shown as an insert in (E). The large arrow indicates the ventral axis. (F) A composite windrose displaying the angles migrated by cells traced in five E10.5 movies (10 cells per movie). Windroses were aligned with respect to the ventral axis (large arrow). The position of the neural tube (n), notochord (no), aorta (a), lumen of the hind-gut (g), near mesentery (nm), and far mesentery (m) are indicated. Note that very few germ cells are present in the far mesentery at E10.5. Such cells do not exhibit directed migration. Scale bar, 58 um. (A) and (D) are in the same scale.

FIG. 4. PGCs that are in the body wall at E10.5 move towards the developing genital ridge. (A) Targeting analysis of an E9.5 film. The explant shown is the same sample that was analyzed in Fig. 3A. Arrows indicate the eventual targets of cells if they were to continue to move in the direction that was traced. Red curves indicate the future positions of the genital ridges. Note that no cell in this explant has targeted a "genital ridge." (B) Targeting analysis of an E10.5 film. The explant shown is the same sample that was analyzed in Fig. 3D. Note that 6 of 10 cells traced in this explant have targeted the "genital ridges." (C) Summary of targeting data. The indicated number of movies were traced (10 cells per movie) and targeting analysis was performed. The graph displays the average number of cells capable of targeting an area defined as the "genital ridge." Error bars indicate the standard deviation between movies. (D) An additional example of an E10.5 slice. This slice shows an unusually high number (thirteen) of PGCs in the mesentery. Although cells in the body wall of this explant moved towards the genital ridges, no cells in the mesentery exhibited directed migration. Scale bar, 72 μm. "Dor." marks the dorsal and "Lat." the lateral axis of the explant.

the explant. Ten cells were traced in this explant and their paths are indicated by black lines. The traced cells moved along both the anterior–posterior and dorsal–ventral axes of the gut and frequently changed directions during migration. For example, the indicated cell (arrow in Fig. 1B) initially moved toward the ventral side of the gut, but then changed direction to move both dorsally and posterially. Despite being obviously motile, no cell was observed leaving the confines of the gut at this stage. Cell velocities were calculated as described (see Materials and Methods). Average and maximum velocity measurements for each cell were then averaged to obtain an overall average velocity of 16.2 μm/h (SD $\pm$ 2.5) and an average maximum velocity of 38.9 μm/h (SD $\pm$ 4.8) for this specimen. Similar results were obtained in one repeat experiment (data not shown).

Figures 1C and 1D show movement in the transverse plane at the same stage. Figure 1C shows a single confocal plane taken at the start of the experiment. A movie of 8 h of development of this slice is provided as supplementary data (movie 1C). When filmed with this orientation, PGC movements along the DV and ML axes were detected; however, movement along the AP axis resulted in some PGCs moving out of focus and these cells were not traced. Figure 1D shows the kinetic tracks of 10 cells moving within this specimen. Similar results were obtained in one other experiment and a summary of germ cell velocity data is presented in Fig. 6.

In this and in similar slices, we have noted that PGCs often appear asymmetrically distributed within the hind-gut at the start of filming (Figs. 1C and 1E) with most PGCs occupying the ventral wall of the gut. Movement of PGCs within these samples disrupts this initial asymmetry and PGCs were frequently found distributed around the entire circumference of the gut after seventeen hrs. in culture (Figs. 1D and 1F). Again, no cell was observed leaving the confines of the hind-gut at this stage.

PGCs Emerge from the Hind-Gut between E9.0 and E9.5

At E9.5, the head, forelimb buds, and one flap of lateral epidermis were dissected away and the trunk and tail of the embryo was cultured to visualize PGC behavior. Figure 2A shows a single confocal image taken in the midsaggittal plane at this stage. A movie of 8 h of development of this specimen is provided as supplementary data (movie 2A). Initially, PGCs were present within the body wall and hind-gut of the embryo, with a high density of cells present at the boundary between the dorsal wall of the gut and the ventral body wall (Fig. 2A). Figure 2B shows the kinetic tracks of 10 cells in this specimen. Cells in the body wall exhibited net movement in the dorsal direction (away from the gut). Likewise, cells within the confines of the gut moved dorsally, and some cells (arrows in Fig. 2B) were observed emerging from the dorsal wall of the gut where it abuts the body wall. The overall average velocity for the specimen shown in Figs. 2A and 2B was 15.3 μm/h (SD $\pm$ 4.0) and the average maximum velocity was 41.5 μm/h (SD $\pm$ 12.6).

Figures 2C and 2D show germ cells moving in a transverse plane within a 200-μm-thick slice sectioned from the trunk of an E9.5 embryo. A movie of this specimen is provided as supplementary data (movie 2C). The movie is rotated 90° counterclockwise in comparison to the still frame image shown in Fig. 2C. Most cells are present within the body wall of this slice with only a few cells remaining in the hind-gut (Fig. 2C). During filming, some of the cells (arrows in Fig. 2D) in the hind-gut moved dorsally and exited the gut into the body wall. Cells in the body wall either moved dorsally or laterally with overall net movement being away from the gut and to the sides. Similar results were obtained in five experiments and germ cell velocity data are summarized in Fig. 6.

Figures 2E and 2F show a comparison between the morphology of cells present in the hind-gut at E9.0 and E9.5. At

FIG. 5. At E11.5, germ cell movements differ between male and female embryos. (A) Example of a genital ridge dissected from an E12.5 female embryo demonstrating the characteristic spotty appearance of the female sex cords. (B) A single optical slice taken from the anterior end of a female E11.5 genital ridge. "Post." marks the posterior and "Med." the medial axis of the tissue. Scale bar, 58 μm. This explant was filmed for 12 h and cell movements are shown in (C). A windrose diagram displaying the angle of movement for each cell traced is shown as an insert in (C). The large arrow in the windrose indicates the posterior axis of the ridge. (D) An example of a genital ridge dissected from an E12.5 male embryo demonstrating the characteristic striped appearance of the male sex cords. (E) A single optical slice taken from the anterior end of a male E11.5 ridge. Scale is the same as in (B). This explant was filmed for 12 h and cell movements are shown in (F). A windrose diagram displaying the angle of movement for each cell traced is shown as an insert in (F). (G) A composite windrose formed by overlaying windroses generated from nine female films. The trajectories of 90 cells are shown (10 cells/movie). (H) A composite windrose formed by overlaying windroses generated from nine male films. The trajectories of 90 cells are shown (10 cells/movie). (I) The trajectories of the germ cells analyzed in (G) and (H) were assigned to four quadrants (Medial–Posterior, Lateral–Posterior, Medial–Anterior, and Lateral–Anterior). The average number of germ cells per movie moving within each quadrant is plotted for male and female ridges. Error bars indicate the standard deviation between films.

FIG. 6. PGCs slow as they approach the genital ridge. Average and average maximum cell velocities were determined in the indicated number of movies (see Materials and Methods). Ten cells were traced per movie at E9.0, E9.5, and E10.5. Twenty cells were traced per movie at E11.5 and E12.5. Error bars indicate the standard error of the mean.

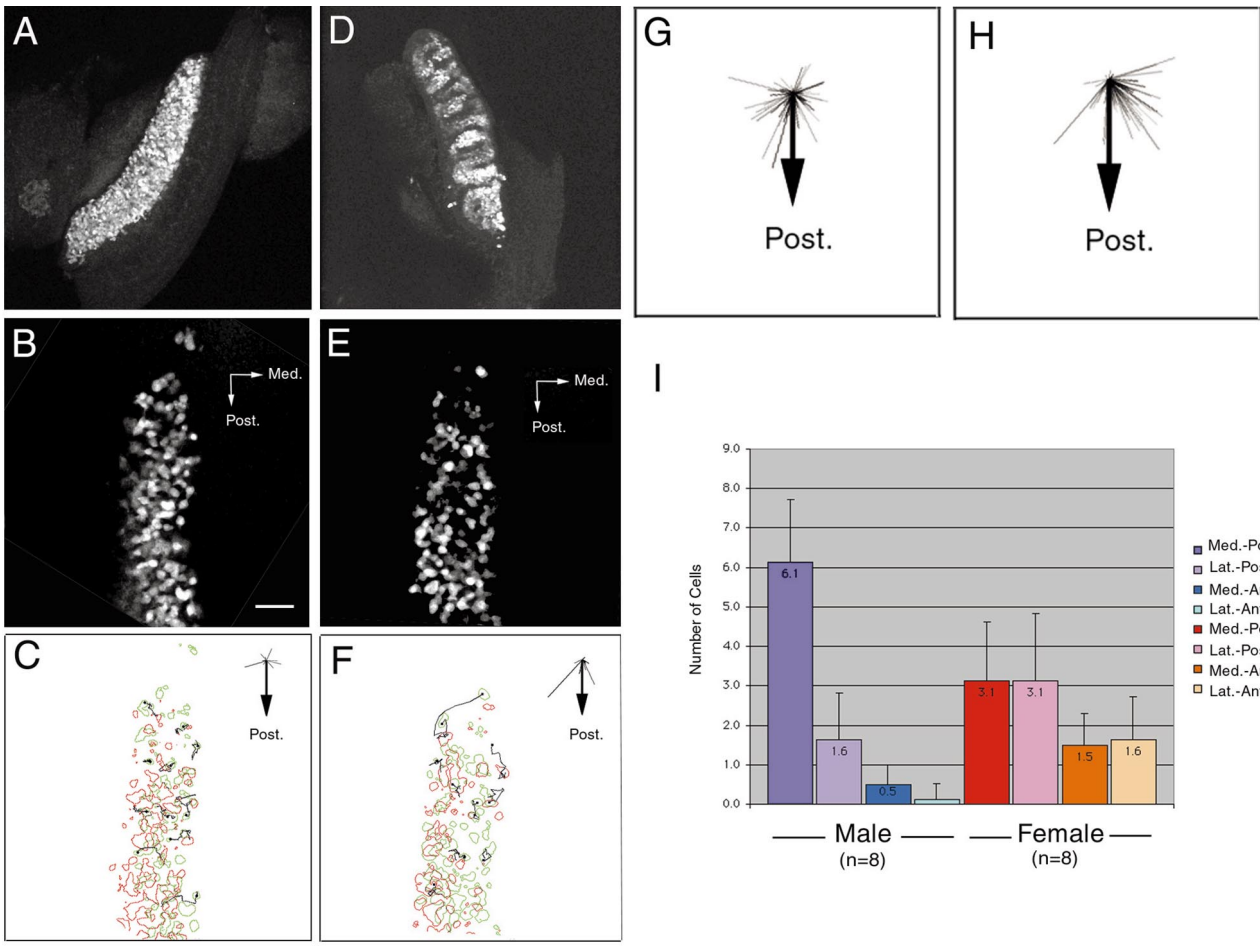

5

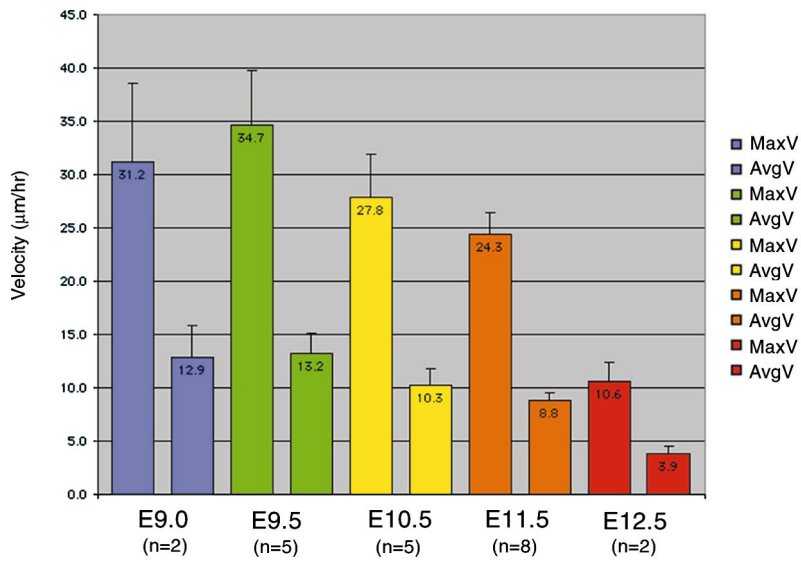

6

both stages, cells were found within the plane of the hind-gut frequently near the basal side of the epithelium. The indicated cell shown in Fig. 2E has extended a process along the basal side of the gut and in a short time-lapse movie (data not shown) was seen to move along the basal side remaining within the confines of the gut. In Fig. 2F, the indicated cell has extended a process away from the gut. In a short time-lapse movie (data not shown), this process was extended and retracted vigorously outside the confines of the gut.

The Angle of PGC Migration Changes between E9.5 and E10.5

Figure 3A shows a single confocal image of a representative 200-μm-thick slice sectioned from the trunk of an E9.5 embryo. A movie of 8 h of development of this specimen is provided as supplementary data (movie 3A). Figure 3B shows the kinetic tracks of 10 cells moving within this specimen. The net trajectory of each cell traced in Fig. 3B was projected onto a common origin to form the windrose shown as an insert in Fig. 3B (see Materials and Methods). In this experiment, all net trajectories make obtuse angles with respect to the axis of the gut (arrow in the windrose diagram), indicating that cells in this experiment moved dorsally (with slight deviations to the sides). Figure 3C shows a composite windrose formed by overlaying the windroses generated from five individual E9.5 films. Of the 50 cells traced in these films (10/film), the majority (30) moved at obtuse angles with respect to the gut. Hence, the majority of the cells are not moving toward the future position of the genital ridges.

In contrast, Figs. 3D and 3E show a similar analysis performed on a representative transverse slice dissected from the trunk of an E10.5 embryo. A movie of this specimen is available as supplementary data (movie 3D). This movie is rotated 90° counterclockwise in comparison to the still frame image shown in Fig. 3D. The image in 3D was rotated in order to display the explant with the same orientation as the E9.5 slice (Fig. 3A). Figure 3F shows a composite windrose formed by overlaying windroses generated from five individual E10.5 films. In the experiment shown in Figs. 3D and 3E, the majority of cells are moving at acute angles and this is also evident in the composite windrose shown in Fig. 3F, where out of the 50 cells traced, 35 were found to move at acute angles with respect to the gut. Hence, at this stage, most germ cells appear to be moving towards the genital ridges.

The windrose analysis is useful for giving an overall impression of degree and direction of PGC movements at different stages of development. However, at E10.5, PGCs moved towards the genital ridges from widely divergent sites (arrows in Fig. 3E). This means that they approach the genital ridges from directions that can vary by as much as 90°, which makes windrose assays less helpful as an indicator of directionality. Instead, we have used the targeting assay illustrated in Fig. 4 to quantitate germ cell behavior at these stages. Figure 4A shows a targeting analysis performed on the same E9.5 experiment that was analyzed in Fig. 3A, and Fig. 4B shows a targeting analysis performed on the same E10.5 experiment analyzed in Fig. 3D. Cell traces were overlaid over inverted gray-scale images representing the final frame of each movie. The starting and ending positions of each trace were connected to generate a line representing the potential target area (indicated by an arrow) for each cell. Cells with target zones within the ventral–lateral edge of the slice (as indicated by red curves in Fig. 4) were scored as having moved towards the "genital ridge." Figure 4C shows a summary of E9.5 and E10.5 targeting data. At both stages, 5 movies were generated and 10 cells per movie were analyzed. At E9.5 an average of 1.8 (SD $\pm$ 1.6) cells out of 10 moved toward the "genital ridge." At E10.5 an average of 6.6 (SD $\pm$ 1.9) cells out of 10 moved toward the "genital ridge." This represents a statistically significant change in cell behavior between E9.5 and E10.5 (t-test, $P = 0.003$).

PGCs Do Not Exhibit Directed Migration in the Mesentery

In conventional descriptions of PGC movement, they are said to emerge from the hind-gut and migrate up the extended mesentery to reach the developing genital ridges. We have never observed this phenomena. Instead, PGCs migrate out of the hind-gut at E9.5 before the mesentery extends and by E10.5 most PGCs are in the body wall (see Figs. 3A, 3D, and 4D). At E10.5, a small number of PGCs are present at the base of the mesentery ("nm" in Figs. 3D and 4D). These cells are capable of exhibiting directed migration and can reach the genital ridges. The few PGCs that remain in the far mesentery move about randomly and often disappear during filming (movie 4D available as supplementary data). These cells do not target the genital ridges. We have examined thirteen additional E10.5 films similar to those shown in Figs. 3 and 4. In our E10.5 films, we have observed a total of 35 cells in the far mesentery. None of these cells were seen to migrate up the mesentery to reach the genital ridges (data not shown).

At E11.5 PGCs Organize into Sex Cords

By E12.5, male and female ridges can be readily distinguished by the appearance of sex cords. In the female, PGCs form small clusters giving the developing ovary a spotty appearance (Fig. 5A); whereas, in the male, PGCs align into stripes (Fig. 5D). To examine how sex cords form, we filmed whole genital ridges dissected from E11.5 male and female embryos. Figure 5B shows a single confocal image taken at the anterior end of a female E11.5 genital ridge, and Fig. 5E shows a confocal image taken from the anterior end of a male ridge. These specimens were filmed for 12 h and movies are available as supplementary data (movies 5B and 5E). Both movies are rotated in comparison to the still frame images shown in Figs. 5B and 5E. The still-frame

images were adjusted to display both genital ridges with the same orientation. The movements of 10 cells were traced in both male and female ridges (Figs. 5C and 5F) and windrose analyses were performed (inserts in Figs. 5C and 5F). In the female ridge, movements appeared random; however, in the male, most PGCs moved posteriorly. Figures 5G and 5H show the composite windroses formed by overlaying windroses generated from eight female (80 cells) and eight male (80 cells) films. In the male, an average of 6.1 (SD ± 1.6) cells out of 10 cells traced per movie exhibited net movement in the medial–posterior quadrant. In the female, movements were more random, with an average of 3.1 (SD ± 1.5) cells out of 10 cells traced per movie exhibiting movement in the medial–posterior quadrant (Fig. 6I). This represents a statistically significant difference in germ cell movements at the anterior end of male and female ridges (*t*-test, $P = 0.0009$). PGC movements at the posterior ends of E11.5 ridges were random in both the male and female (data not shown).

The Velocity of PGCs Is Developmentally Regulated

Figure 6 shows a summary of the velocity data collected from various stages of germ cell development. The average and maximum velocity measurements from the indicated number of movies were compared. At E9.0 and E9.5, germ cells are moving quickly with average velocities of 12.9 (SEM ± 3.0) and 13.2 (SEM ± 1.9) μm/h. At E10.5, germ cells are moving slightly slower with an average velocity of 10.3 μm/h (SEM ± 1.5) and this slowing trend continues with E11.5 germ cells exhibiting an average velocity of 8.8 μm/h (SEM ± 0.7) and E12.5 germ cells exhibiting an average velocity of 3.9 μm/h (SEM ± 0.63). At all stages, germ cells exhibited spurts of faster movement with maximum velocities being approximately 2.5 times the average. Both average and maximum velocities slow as germ cells colonize the genital ridges (E12.5).

DISCUSSION

We have shown that mouse germ cells are continuously motile from E9.0 until E12.5, but differences exist in both the velocity and directionality of germ cell motility at different stages. Four clearly distinct phases can be recognized, which must define corresponding spatiotemporal controls on PGC motility. First, at E9.0, germ cells move rapidly, but are confined to the hind-gut. Second, at E9.5, germ cells emerge from the hind-gut and invade the body wall before the mesentery forms. At this stage, germ cells move dorsally and do not appear to be targeting the future sites of the genital ridges. Third, at E10.5, PGCs move directionally towards the genital ridges from widely divergent starting positions in the dorsal body wall and base of the mesentery. The few germ cells that remain in the hind-gut mesentery do not move directionally and often disappear during filming. Finally, at E11.5, most germ cells have reached the genital ridges and their movements are slowing. In the female, PGC movements at E11.5 appear random. In the male, however, the majority (61%) of germ cells that were traced were moving in the medial–posterior direction.

The most general finding of this study is that PGCs are actively motile throughout most or all of the time between their formation and gonad formation. This is consistent with previous observations on fixed tissue samples and on culture experiments. The morphology of PGCs in fixed tissue has suggested that PGCs are actively migratory from E9.0 until E12.5 (Clark and Eddy, 1975). PGCs isolated from E8.5 (Godin *et al.*, 1990) and E10.5 (Donovan *et al.*, 1986) can migrate on feeder layers in culture whereas PGCs isolated from E11.5 embryos do not (Donovan *et al.*, 1986). The velocity measurements obtained in culture experiments of mouse (Donovan *et al.*, 1987) or *Drosophila* PGCs (Jaglarz and Howard, 1995) were generally higher than the velocity measurement that we have obtained for PGCs migrating in tissue. This probably reflects the physical restraints imposed on PGC movement by ECM or other cells present in tissue that are absent in disassociated cell culture.

It is possible that PGCs are motile continuously from gastrulation until gonadogenesis. Anderson *et al.* (2000) have observed live PGCs moving in tissue isolated from E8.0 embryos. At this stage, PGCs actively migrate out of the primitive streak and move into the endoderm. There is, however, a small window of time during which we have been unable to directly observe PGC behavior in tissue. This is between E8.5 and E9.0, where the morphogenetic movements of the embryo (e.g., turning) make it difficult to keep PGCs in focus during filming. The morphology of PGCs in the hind-gut pocket has suggested that they may be nonmotile during this period (Anderson *et al.*, 2000; Clark and Eddy, 1975; Spiegelman and Bennett, 1973; and our personal observations). If this is the case, some signal must instruct the PGCs when to stop moving after gastrulation and when to start moving again. Alternatively, if germ cells are continuously motile until colonization of the gonad, then fencing mechanisms (for example, their restriction to the hind-gut at E9.0) are key factors in controlling germ cell targeting.

At E9.0, PGCs are clearly motile. At this time point, PGCs are initially present within the ventral wall of the hind-gut and their movements result in the redistribution of these cells around the entire circumference of the gut. PGCs were also restrained within the confines of the gut suggesting that the outer boundary of the gut presents a barrier to their movements. By E9.5, PGCs were no longer constrained by the boundary of the hind-gut. They emerged from the dorsal side of the gut and moved rapidly into the body wall. In *Drosophila*, PGCs emerge from the ventral side of the gut (Warrior, 1994) and this process is thought to be preceded by physical changes in the structure of the midgut epithelium (Callaini *et al.*, 1995; Jaglarz and

Howard, 1994) as well as a repulsive signal received from the gut (Zhang *et al.*, 1997). The movement of mouse PGCs at E9.5 suggests that they are either being driven by repulsive factors from the gut or attractive forces from the entire dorsal body wall.

In the conventional model of PGC development, germ cells are thought to be physically integrated into the hind-gut epithelium and are released from the epithelium by undergoing an epithelial–mesenchymal transition. We now show that PGCs are already motile (mesenchymal) in the hind-gut, before being released at E9–E9.5. Additionally, we have previously shown that PGCs in the hind-gut do not express the epithelial marker E-cadherin, but turn on its expression after they leave (Bendel-Stenzel *et al.*, 2000). Hence, germ cell release from the hind-gut is not a typical epithelial–mesenchymal transition.

At E9.5, there is no net movement of PGCs toward the sites of the genital ridges. By E10.5, however, germ cells clearly home in on the genital ridges from widely divergent starting positions. This suggests either that an attractive signal from the genital ridges comes on at E10–E10.5, or its receptor comes on in the PGCs at this time. We can address this in future experiments by recombining PGCs and tissues from different stages of development.

The behavior of E10.5 PGCs allows us to reconsider conventional models for germ cell migration. It has been proposed that PGCs may move randomly and simply become trapped by somatic tissue of the ridge in a manner similar to that proposed for PGC trapping in the chick embryo (Kuwana and Rogulska, 1999). Also, it has been proposed that PGCs may not be actively migratory, but might be passively carried to the ridge by the movements of surrounding tissue. The directional migration of PGCs at E10.5 makes these two models unlikely. It has also been proposed that PGC–PGC contact might also play a role in germ cell migration by a process of coalescence (Gomperts *et al.*, 1994), a view reinforced by the effects of blocking antibodies against E-cadherin (Bendel-Stenzel *et al.*, 2000). At E10.5, we frequently observed germ cells making and breaking contacts with other PGCs, but some PGCs appeared capable of independently migrating towards the genital ridges. The resolution of our films was not sufficient to evaluate whether such cells remained in contact with other PGCs via very long, thin processes. Hence, we are not able to definitely assess the relative importance of coalescence and individual migration in this process. It is likely that both play a role.

Previous experiments on cultured PGCs have suggested either a chemotactic mechanism (Godin *et al.*, 1990; Godin and Wylie, 1991) or an extracellular matrix gradient mechanism (Alvarez-Buylla and Merchant-Larios, 1986; Ffrench-Constant *et al.*, 1991) for PGC guidance. The behaviors of PGCs in the movies shown here do not discriminate between these. However, they show that whatever the mechanism, it is relatively short-ranged. We have examined 15 E10.5 films (see Figs. 3D and 4D for examples). From these films we have observed a total of 35 cells in the hind-gut mesentery. None of these cells were seen to migrate up the mesentery to reach the genital ridges. Typically, cells with in the mesentery moved about randomly before becoming fragmented and disappearing.

Conventionally, PGCs are described as migrating from the gut, along the mesentery, round the angles of the dorsal body wall, and laterally into the genital ridge. Static images of PGCs in Oct4ΔPE:GFP animals suggest the same scenario. At E10.5, PGCs in Oct4ΔPE:GFP mice are present in the same positions as PGCs in other strains. At E10.5, they are found scattered around the gut and mesentery as well as in the body wall (see Fig. 4D and Bendel-Stenzel *et al.*, 2000 for examples). However, time-lapse analysis reveals that cells in the far mesentery do not migrate towards the genital ridges. It is a formal possibility that cutting slices from the trunk of the embryo disrupts long-range signals required for PGC migration. However, we have been unable to culture and film whole embryos in order to test this hypothesis. From the data presented here, we suggest that PGCs are released from the gut before mesentery formation, but they continue to leave the gut as it moves away from the dorsal body wall. As the mesentery extends, PGCs eventually become unable to respond to signals from the genital ridges and only those PGCs present in the body wall and root of the mesentery colonize the developing gonads. PGCs further away remain ectopic and may die. Hence, PGC migration appears to be an inefficient process that selects many, but not all of the PGCs for entry into the developing gonad.

By E11.5, PGCs in the region of the genital ridges are moving more slowly, and during the next 24 h become organized into sex cords. PGCs in the male exhibit more orderly movements than cells in the female. These movements may contribute to the process of sex determination. Sex determination in mammals is orchestrated by the somatic tissue of the gonad. (Buehr *et al.*, 1993); hence, the orderly movements of PGCs observed in the male at E11.5 are most likely a physical manifestation of the organizing influence of the surrounding cells in the developing testes.

In summary, this study is the first to provide a detailed and quantitative analysis of the behavior of live PGCs in mammalian tissue. These observations demonstrate that PGCs are actively motile from E9.0–E12.5 of mouse development and exhibit four distinct phases of behavior. These four phases of PGC behavior are similar to the stages of PGC development as defined by observation and genetic screens in *Drosophila* (Moore *et al.*, 1998; Warrior, 1994). This study should serve as a useful baseline for assaying growth factors that affect PGC motility and for quantitatively addressing the effects of mutations on the process of PGC migration.

ACKNOWLEDGMENTS

We thank Bob Hennigan for training on the confocal and Cathy Krull for advice on live cell microscopy. We thank Matt Kofron for

assistance with the cell tracing. This work was supported by funding from the NIH (NRSA fellowship 1 F32 HD008678-01 (to K.M.) and RO1 HD33440-01 (to C.W.).

REFERENCES

Alvarez-Buylla, A., and Merchant-Larios, H. (1986). Mouse primordial germ cells use fibronectin as a substrate for migration. *Exp. Cell Res.* **165,** 362–368.

Anderson, R., Copeland, T. K., Scholer, H., Heasman, J., and Wylie, C. (2000). The onset of germ cell migration in the mouse embryo. *Mech. Dev.* **91,** 61–68.

Anderson, R., Fassler, R., Georges-Labouesse, E., Hynes, R. O., Bader, B. L., Kreidberg, J. A., Schaible, K., Heasman, J., and Wylie, C. (1999). Mouse primordial germ cells lacking beta1 integrins enter the germline but fail to migrate normally to the gonads. *Development* **126,** 1655–1664.

Bendel-Stenzel, M. R., Gomperts, M., Anderson, R., Heasman, J., and Wylie, C. (2000). The role of cadherins during primordial germ cell migration and early gonad formation in the mouse. *Mech. Dev.* **91,** 143–152.

Buehr, M., McLaren, A., Bartley, A., and Darling, S. (1993). Proliferation and migration of primordial germ cells in We/We mouse embryos. *Dev. Dyn.* **198,** 182–189.

Callaini, G., Riparbelli, M. G., and Dallai, R. (1995). Pole cell migration through the gut wall of the Drosophila embryo: Analysis of cell interactions. *Dev. Biol.* **170,** 365–375.

Clark, J. M., and Eddy, E. M. (1975). Fine structural observations on the origin and associations of primordial germ cells of the mouse. *Dev. Biol.* **47,** 136–155.

Donovan, P. J., Stott, D., Cairns, L. A., Heasman, J., and Wylie, C. C. (1986). Migratory and postmigratory mouse primordial germ cells behave differently in culture. *Cell* **44,** 831–838.

Donovan, P. J., Stott, D., Godin, I., Heasman, J., and Wylie, C. C. (1987). Studies on the migration of mouse germ cells. *J. Cell Sci. Suppl.* **8,** 359–367.

Ffrench-Constant, C., Hollingsworth, A., Heasman, J., and Wylie, C. C. (1991). Response to fibronectin of mouse primordial germ cells before, during and after migration. *Development* **113,** 1365–1373.

Godin, I., Wylie, C., and Heasman, J. (1990). Genital ridges exert long-range effects on mouse primordial germ cell numbers and direction of migration in culture. *Development* **108,** 357–363.

Godin, I., and Wylie, C. C. (1991). TGF beta 1 inhibits proliferation and has a chemotropic effect on mouse primordial germ cells in culture. *Development* **113,** 1451–1457.

Gomperts, M., Garcia-Castro, M., Wylie, C., and Heasman, J. (1994). Interactions between primordial germ cells play a role in their migration in mouse embryos. *Development* **120,** 135–141.

Hogan, B., Beddington, R., Constantini, F., and Lacy, E. (1994). "Manipulating the Mouse Embryo." Cold Spring Harbor Press, Cold Spring Harbor, NY.

Jaglarz, M. K., and Howard, K. R. (1994). Primordial germ cell migration in *Drosophila melanogaster* is controlled by somatic tissue. *Development* **120,** 83–89.

Jaglarz, M. K., and Howard, K. R. (1995). The active migration of Drosophila primordial germ cells. *Development* **121,** 3495–3503.

Krull, C. E., and Kulesa, P. M. (1998). Embryonic explant and slice preparations for studies of cell migration and axon guidance. *Curr. Top. Dev. Biol.* **36,** 145–159.

Kuwana, T., and Rogulska, T. (1999). Migratory mechanisms of chick primordial germ cells toward gonadal anlage. *Cell. Mol. Biol.* **45,** 725–736.

Moore, L. A., Broihier, H. T., Van Doren, M., Lunsford, L. B., and Lehmann, R. (1998). Identification of genes controlling germ cell migration and embryonic gonad formation in Drosophila. *Development* **125,** 667–678.

Spiegelman, M., and Bennett, D. (1973). A light- and electron-microscopic study of primordial germ cells in the early mouse embryo. *J. Embryol. Exp. Morphol.* **30,** 37–118.

Stott, D., and Wylie, C. C. (1986). Invasive behavior of mouse primordial germ cells in vitro. *J. Cell Sci.* **86,** 133–144.

Warrior, R. (1994). Primordial germ cell migration and the assembly of the Drosophila embryonic gonad. *Dev. Biol.* **166,** 180–194.

Zhang, N., Zhang, J., Purcell, K. J., Cheng, Y., and Howard, K. (1997). The Drosophila protein Wunen repels migrating germ cells. *Nature* **385,** 64–67.

Received for publication May 21, 2001
Revised July 26, 2001
Accepted August 2, 2001
Published online November 14, 2001